JOURNAL OF CATALYSIS 143, 409–429 (1993)

Scanning Tunneling Microscopy Study of Pd Thin Film Catalyst

I. Effect of the Adsorbates and Surface Reaction on the Film Structure

KING LUN YEUNG AND E. E. WOLF

Department of Chemical Engineering, University of Notre Dame, Notre Dame, Indiana 46556

Received September 28, 1992; revised December 22, 1992

A 25-nm Pd thin film catalyst supported on HOPG was used to study the effect of adsorbates and surface reaction on the surface microstructure. The effect of the hydrogen and helium treatment at 523 K on the evolution of the film structure with time shows that the reactive hydrogen affects a greater change in the film structure than helium. The effect of C_4 hydrocarbons (*n*-butane, 1-butene, and 1,3-butadiene) and treatment temperature on the film microstructure was also examined. The hydrocarbons that have a strong catalytic interaction with the Pd film will preferentially dehydrogenate and cause a large change in the film structure. During the reaction of C_4 hydrocarbons with hydrogen over the Pd thin film catalyst, the more reactive hydrocarbons cause a large structural transformation regardless of the reaction, whether it is 1,3-butadiene hydrogenation or *n*-butane dehydrogenation. The results show that surface reactions and reactive gases have a strong effect on the Pd film structure, and that the activity and selectivity of the film catalyst are strongly dependent on its surface structures.

INTRODUCTION

The ability of the scanning tunneling microscope (STM) in imaging 3-dimensional surface features with subnanometer resolution (*1*, *2*) has resulted in a significant growth in the application of the STM in the area of catalyst characterization (*3–13*). STM has been used to image the surface structures of different catalytic systems, both clean and adsorbate covered surfaces, from single crystals (*3*, *4*) to polycrystalline foils (*5*), and from thin films (*6*, *7*) to small clusters (*8*, *9*). However, most of the studies were conducted on model surfaces, and the relationship between structure and catalytic activity has not been addressed in most of the publications.

The effect of both reactive and inert gases on the surface microstructure of the catalytically active materials is reported in this paper. The obvious choice for the catalytic system is supported metal particles; however, our earlier STM studies on supported catalysts on graphitic substrates (*10–13*) showed that even in a simplified system the supported catalysts exhibit complex surface morphologies. The catalyst particles exhibit both size and shape distributions and are strongly affected not only by the treatment gases, but also by the choice of precursor, support, preparation, and by the pretreatment history of the catalyst. Due to these complicating factors, it is difficult to establish the relationship between the catalyst structure and its activity.

The use of the thin film catalyst reported in this work offers the potential of reducing the number of physical variables to that of the film thickness and the microstructure in two dimensions. A Pd thin film catalyst was prepared by physical deposition of pure Pd onto a graphite substrate under high vacuum. The evolution of the film microstructures (vs time) during the hydrogen and helium treatment was studied to determine the effect of the hydrogen and inert gases on the surface microstructure of the Pd film. The effect of the C_4 hydrocarbons, *n*-butane, 1-butene, and 1,3-butadiene, on the

0021-9517/93 $5.00

film microstructure was also studied. In addition, the effect of the surface reaction on the microstructure was also studied by exposing the thin film catalyst to a reactant mixture of hydrogen and C_4 hydrocarbons at different reaction temperatures.

EXPERIMENTAL

Pd Film Preparation and Pretreatment

Thin film preparation. A supported thin film catalyst was prepared by evaporating 14 mg (corresponding to about 25 nm film thickness according to the calibration of the evaporator) of Pd wire at 1×10^{-6} Torr onto highly oriented pyrolytic graphite (HOPG) in a vacuum evaporator (Denton DV-502). In each batch of deposition, six samples were placed in a tilted (30°) platform to allow uniform deposition of the metal, giving a Pd loading of about 0.05 $\mu g/cm^2$. Each Pd/HOPG sample has a dimension of 1.2×1.2 cm^2, and four of the thin film catalysts were used in this study. Prior to each experiment the microstructure of the deposited Pd thin films were imaged with the STM, and they were found to be reproducible within the six samples prepared in the same batch.

H_2 and He pretreatment. Pd thin film catalysts of 0.6×1.2 cm^2 were used in each of the pretreatment and reaction studies. The H_2 treatment study was conducted in quartz tube reactor (1.50 cm I.D.) at 523 K and 1 atm, and a H_2 flowrate of 120 ml/min. The hydrogen used in the study was further purified by passing it through a zeolite/drierite column to remove hydrocarbon contaminants and moisture, and through an oxygen trap (Alltech Associates) to remove the remaining oxygen from the gas stream. To study the evolution of the film microstructure as a function of time, the H_2 treatment was interrupted and the film catalyst was quenched to room temperature at various time intervals for STM analysis at ambient condition. Since repeated exposure to air occurred during the study, the catalyst was flushed with Ar and then with H_2 (room temperature) prior to continuing the subsequent treatment to minimize the effect of adsorbed O_2 or H_2O on the surface. A similar He annealing treatment was conducted at 523 K in flowing He to study its effect on the evolving film microstructure. The helium used in the treatment and the argon used in purging the samples are purified in similar manner as the H_2 gas to reduce contaminants.

Pretreatment in C_4 hydrocarbons. The effect of C_4 hydrocarbons on the film microstructure was also studied for *n*-butane, 1-butene, and 1,3-butadiene. A low concentration of hydrocarbons was used to minimize carbon deposition on the catalyst surface. The hydrocarbons (HC) were diluted in nitrogen to give a HC partial pressure of 4 Torr at a total pressure of 1 atm. The HC treatment was conducted in a smaller quartz tube reactor (0.80 cm I.D.) at an overall gas flowrate of 110 ml/min. The thin film catalyst was then sequentially treated at 348 and 473 K for 90 min each, and the film structures were analyzed with the STM at ambient conditions. Prior to the treatment and after quenching, the film catalyst was flushed with N_2 to remove unwanted surface contaminants.

Surface reaction. To study the effect of surface reaction on the film microstructure, the thin film catalysts were exposed to a reactive mixture of hydrogen and C_4 hydrocarbons at reaction temperatures of 348, 423, and 473 K. The film catalyst was reacted at each selected temperature for 90 min, then it was quenched, and the film microstructures were analyzed with the STM at ambient conditions. The reaction was conducted in a quartz tube reactor (0.80 cm I.D.), and a hydrocarbon concentration of 4 Torr(/760) and a hydrogen-to-hydrocarbon ratio (H_2/HC) of 125 was used with the nitrogen as the diluent gas to give a total flowrate of 110 ml/min.

On the Pd catalyst, 1,3-butadiene is hydrogenated in the presence of hydrogen forming a significant amount of butane and C_4 olefins (1-butene, *cis*- and *trans*-2-butenes). To study the effect of the microstructure on the catalytic behavior of the Pd thin film catalyst, the 1,3-butadiene conversion of each of the structures was compared at

323 K. The reaction was carried out in a quartz flow reactor (1 atm), and the reaction products were separated in a gas chromatograph using a 7-ft chromatographic column packed with 0.19% picric acid/graphpac packings (Alltech Associates, Inc.). The products were monitored with an FID detector.

Scanning Tunneling Microscopy

The STM used in this study is a commercial Nanoscope II (Digital Instrument, Inc.) operated at ambient conditions. Two STM heads of different scanning ranges were employed, a short scan head of 500-nm range and a medium scan head of 7500-nm range. Pt/Ir tips supplied by Digital Instrument were used in this study. Only the tips that can achieve atomic resolution on HOPG were used, and after each study the tips were evaluated in similar manner. The STM was operated in the height imaging mode to provide good morphological information and in current imaging mode to give high-resolution atomic images. The operational bias voltage was kept between 50 and 150 mV with the tunneling current fixed at 1 nA. The horizontal scan frequency was maintained below 5.0 Hz for the best image resolution.

Care was taken to obtain unbiased results from the STM imaging by probing four different regions in each sample, each separated by 0.1 to 0.4 cm. In each region, we mapped the surface morphology by moving the scan area (1000^2 or 500^2 nm^2) in a sequential manner. The images were then analyzed to obtain an average size of the surface features and film thickness. Smaller or larger scans were also obtained to analyze small-scale structures or long-range ordering in film structure. All of the STM images shown in this paper are selected to be representative of the sample's surface morphology as obtained in the study.

Materials

The Pd wire used in the film preparation was 99.999% purity (Johnson Matthey, AESAR), and the HOP graphite was ZYH grade (UCAR Carbon Company, Inc.). The H_2, He, Ar, and N_2 used in this study were UHP quality (Linde Union Carbide). The C_4 hydrocarbons, *n*-butane (99.5%), 1-butene (99.0%), and 1,3-butadiene (99.5%), were supplied by Mattheson Gas Products.

RESULTS

I. Evolution of the Film Microstructure during H_2 Treatment

Figures 1a and 1b show the microstructures of the initial Pd film prior to the H_2 treatment in areas of 1000 and 400 nm size. The film is made up of densely packed, ellipsoidal grains (aspect ratio = 1.2) of 15 nm size (Fig. 1b) forming a thin, uniform film that covers the surface of the graphite. Occasional thin rifts (Fig. 1a) on the film are seldom longer than 5 grains (<80 nm) with the width of about 7 nm or less. The film is made up of two or more layers of grains and has an overall thickness of ~25 nm as measured by the STM.

During the early stages of H_2 treatment (up to 6 h), most of the changes were confined to grain size, which increased continuously with the treatment time. The growth of the grain size introduced nanometer scale roughness to the film. Figure 1c shows that the film appears to maintain its initial structure, covering the substrate's surface with a uniform but rough (~25 nm) layer of Pd. Although the 2-D film structure remains nearly intact after 6 h of H_2 treatment, some localized tears on the film and formation of holes were observed (Fig. 1d). The holes have approximately the size of 1–2 Pd grains, while the tears are much larger and have irregular shapes. Some areas of the sample also exhibit a small degree of grain coalescence and sintering, but these are not frequently observed.

After 15 h of H_2 treatment, the Pd film develops extensive "chain-like" structures, as shown in Fig. 1e. The chains are made up of "links" that are shaped like "commas" and are arranged head to tail to form the long, parallel chain structures. The

"links" (350 × 250 nm) are made up of agglomerated grains that can be seen more clearly in Fig. 1f. The average grain size is 45.41 nm, which is only 3 nm larger than the grain size of the previous 6-h treated film, indicating that the grain growth is playing a relatively minor role in the formation of these chain-like film structures. Figure 1f also shows a peculiar columnar structure of the grains along the axis perpendicular to the film surface which are not evident in both the freshly deposited film and during the early stages of the H_2 treatment (<6 h).

Further H_2 treatment of the Pd film to 32 h resulted in significant changes in the film microstructure. Figure 2a shows a 2000 nm^2 area of the film which starts to form elongated structures of rectangular shape with its surfaces heavily decorated with small triangular particles. Figure 2b shows a closer view of these particles. Although surface decoration with particles is present, the surfaces of these rectangular structures are smooth and the surface structure cannot be detected at this magnification.

While some areas look like facets, most of the film has a similar microstructure as that observed during the early stages of H_2 treatment, but with larger grains due to sintering and coalescence. The grain structures in these regions of the film show two types of sintering processes. Figure 2c shows an area of the film exhibiting a predominant end to end sintering of the grains (usually 2–3 grains in length) forming elongated structures with average dimension of 147.6 × 93.8 nm. The other type of grain structure shown in Fig. 2d is more elliptical in shape and has faint boundaries seen on the surfaces of the grains, indicating that sintering occurs side by side along the minor axis of the grains. These grain structures have an average size of 76.7 nm and an aspect ratio of 1.2. The film also has more openings, which appear to coincide and run parallel with the underlaying steps on the HOPG substrate.

After 48 h of treatment, the continued growth of the elongated structures resulted in well oriented facets. The facets are long and needle-like with aspect ratio ranging from 2 to 8 as shown in Figs. 3a and 3b. The average dimensions of the facets are 308.6 × 112.6 nm (aspect ratio = 2.8). About 20% of the facets have an average size of 492.4 × 230.3 nm (aspect ratio = 2.2) and the rest are ~262.6 nm × 83.2 nm in dimension (aspect ratio = 3.2). The triangular decorations previously seen on the surface of the facets are not seen, and the previous grain structures have annealed out, leaving a smooth surface. However, the faint scar marks from sintering that occur along the length of the facets can still be seen in Fig. 3b.

At this stage of the film treatment (15–48 h), a progressive coalescence and sintering of the grains, with the formation and growth of facets, is observed. As the grains sinter and facets grow, the film ruptures and redisperses. This can indeed be observed in Figs. 3c and 3d after the Pd film was treated in H_2 for 60 h. The disappearance of the facets leaves a disordered and porous-like film structure (Fig. 3c) with an average grain size of 82 nm.

When the film is treated up to 80 h, extensive film fragmentation and particle formation occur as shown in Figs. 3e and 3f. Most of the film fragmentation occurs along the edges of the HOPG substrates with noticeable shrinkage of the film area. These film fragments are highly disordered (Fig. 3f) due to the extensive breakup and are structurally similar to that of the ruptured film shown in Figs. 3c and 3d. Figure 3f shows

FIG. 1. Large and small scale STM images of (a, b) freshly deposited Pd film, (c, d) film structure after 6 h of H_2 treatment, and (e, f) the formation of chain-like structure after 32 h of H_2 treatment at 523 K.

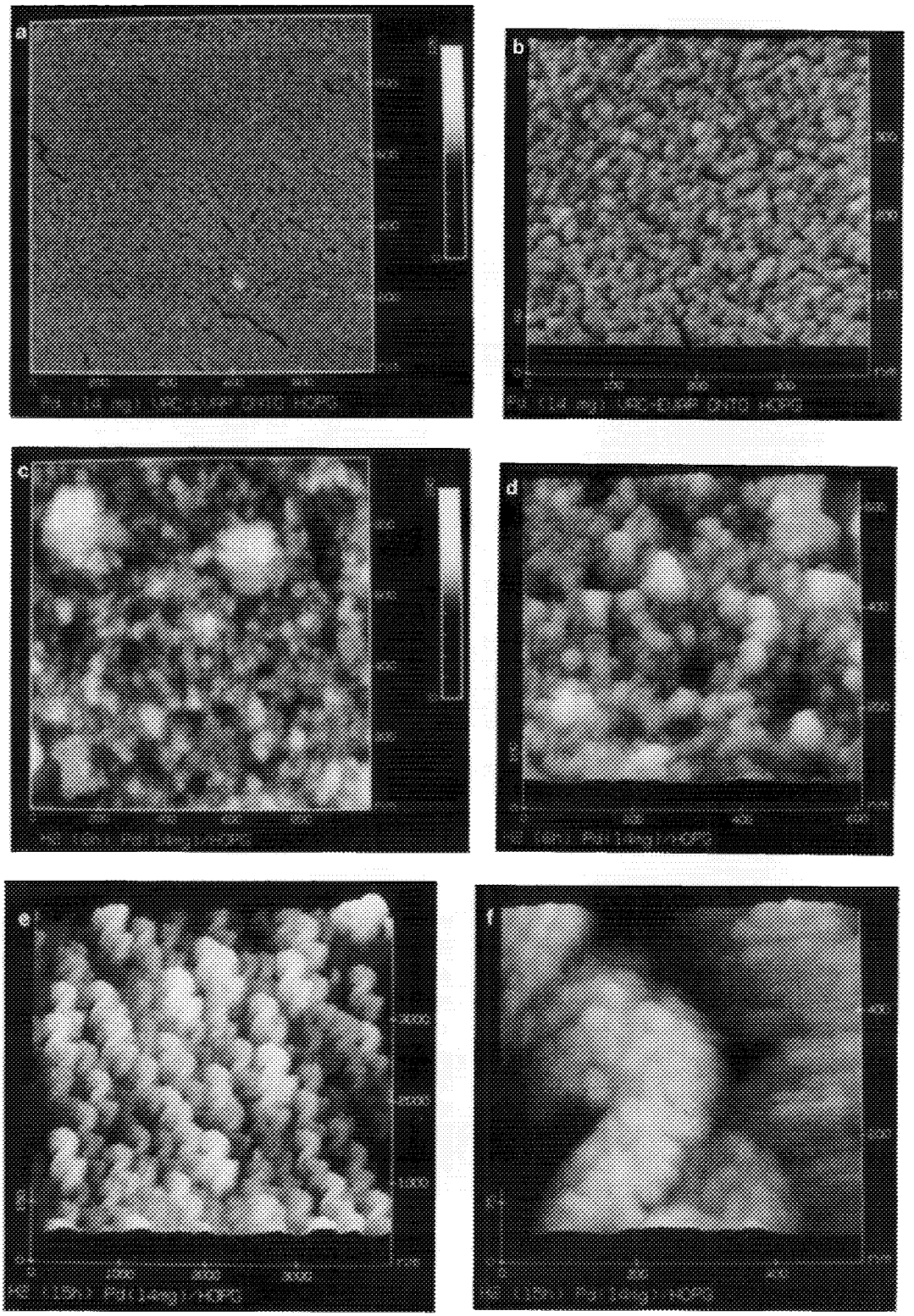
a
b
c
d
e
f

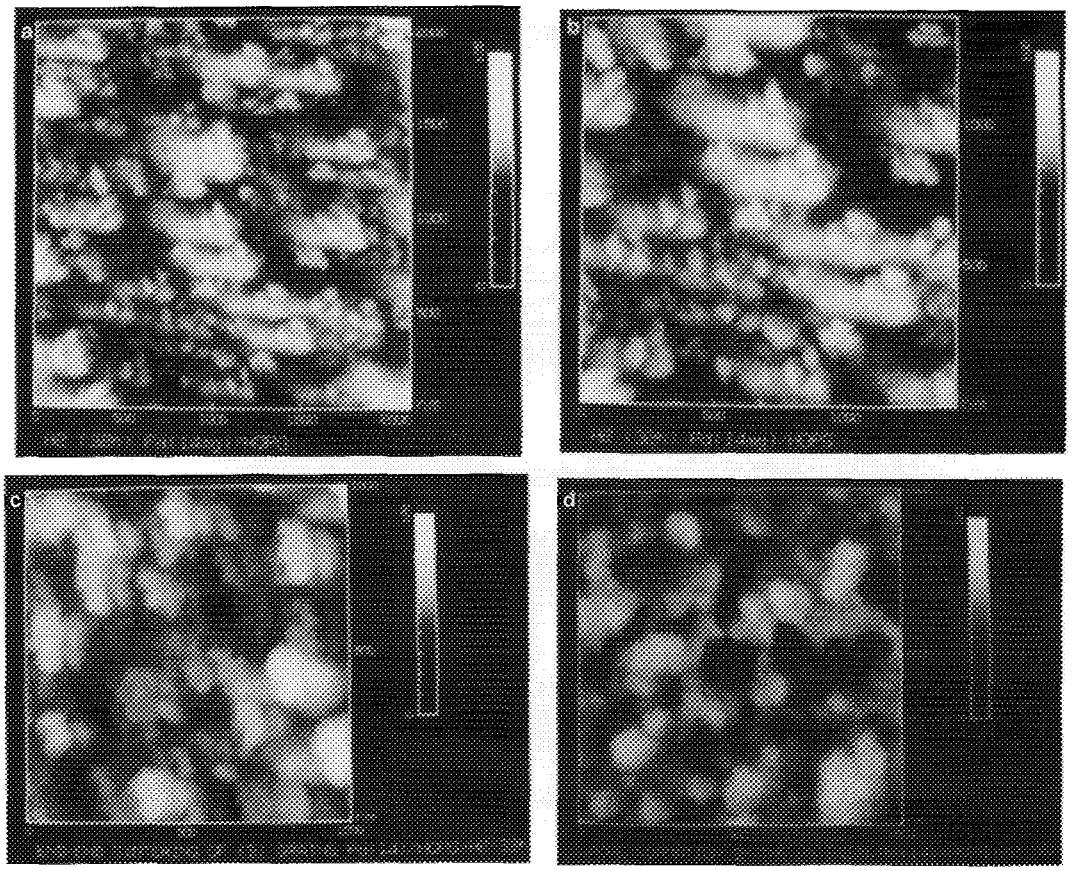

FIG. 2. Film structure after 32 h of H_2 treatment: (a) 2000 × 2000 nm image of the surface facets, (b) a higher magnification image of the facet structure, (c) end-to-end sintering of the Pd grains, and (d) grain coalescence and sintering.

that the formation of the particles from the two-dimensional film was via coalescence and sintering of the Pd grains. The particles are in the early stages of growth and are still attached to the film. The average sizes of the particles are 420 nm with a density of about 30 particles per 1000 × 1000 nm STM scan area. Further treatment of the film in H_2 up to 120 h shows little change in the film structures, and the size of the particles remain unchanged.

These results show that during the course of the H_2 treatment, the Pd/HOPG film undergoes tremendous changes in microstructure. The grains first grow from 15 to 41 nm, while the overall structure of the film does not change greatly. Thereafter, the film morphology experienced significant transformations, formation of chain structures and rectangular facets, until the film ruptured, leading to the formation of a disordered, three-dimensional structure which eventu-

FIG. 3. Large and small scale STM images of the film structure: (a, b) after 48 h, (c, d) 60 h, and (e, f) 80 h of H_2 treatment at 523 K.

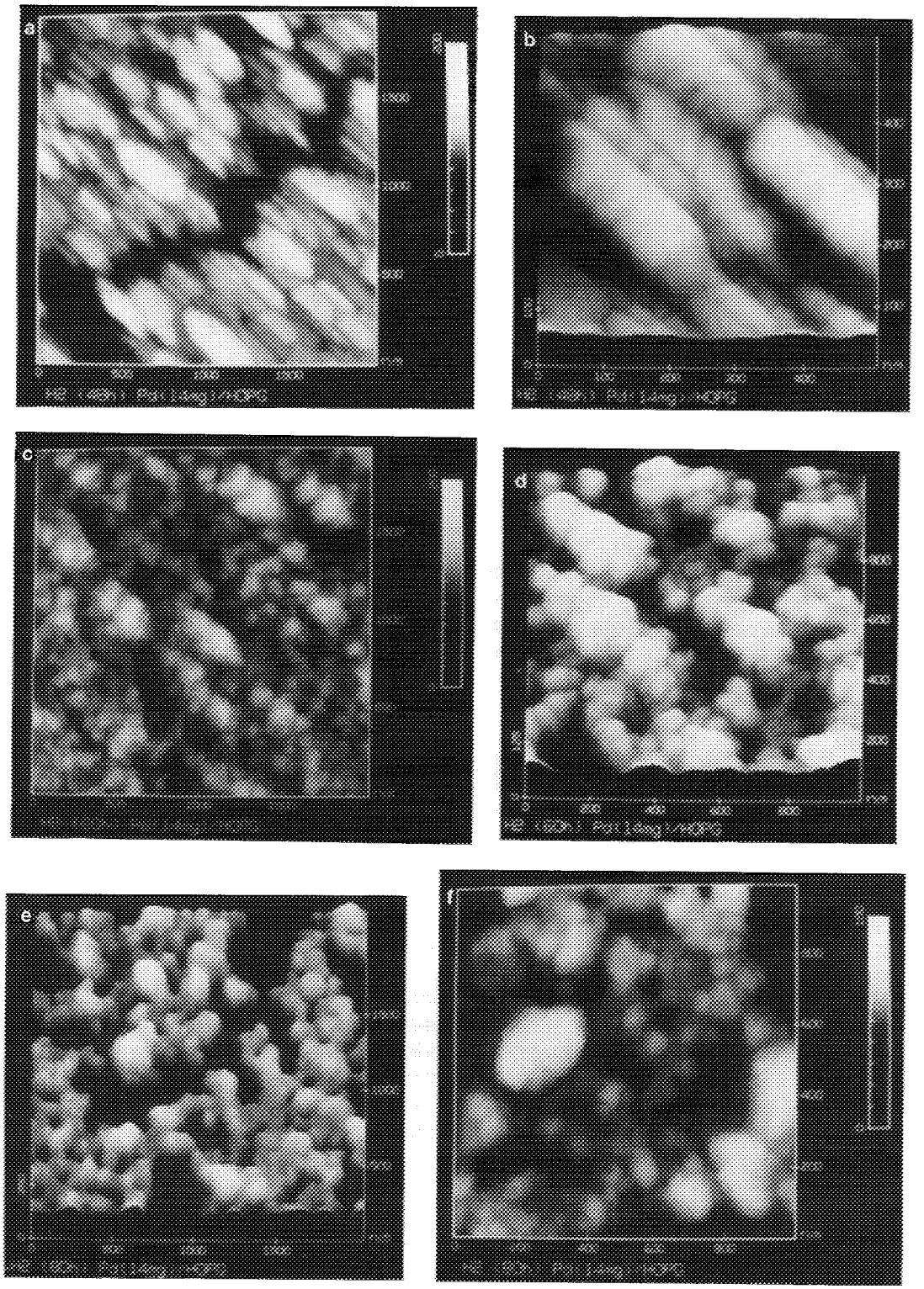
a
b
c
d
e
f

TABLE 1

The Size and Aspect Ratio of the Film Structures Obtained during the H_2 Treatment of the Pd Thin Film at 523 K

Reduction time (h)	Surface structure	Grain and structure size (nm)	Aspect ratio	Film thickness (nm)
0	Grains	15	1.2	25
3	Grains	26	1.2	25
6	Grains + sinter	41	1.3	25
15	Chain-like	350 × 250	1.4	30
	Grains	45.41	1.2	
32	Facets	450 × 200	2.25	32
	Sintered grains			
	Grain 1	147.6 × 93.8	1.6	
	Grain 2	76.7	1.2	
48	Facets			
	Broad facet	492.4 × 230.3	2.2	—
	Narrow facet	262.6 × 83.2	3.3	
60	Grains	82	1.1	35
80	Particles	420	1.3	45

ally forms into separate, large particles. Table 1 summarizes the size and shape (aspect ratio) of the various film structures, and STM measurement of the film thickness during the H_2 treatment.

II. Evolution of the Film Microstructure during He Treatment

Starting with a new Pd film, Fig. 4 shows the evolution of Pd film microstructures during annealing in helium at 523 K for 6, 32, and 60 h. Figures 4a and 4b show large-scale (2000 nm) and smaller scale (500 nm) structures of the Pd film after 6 h of annealing in He. The large scale image (Fig. 4a) shows that the film surface has many large, globular particles with an average size of 78 nm. A closer examination of the film structure (Fig. 4b) shows that these particles are actually surface protuberances (hillocks) made up of agglomerated Pd grains. The grains from either the hillocks or the flat film have a similar size of 21 nm, indicating a growth of only ~6 nm during the 6 h of the He treatment. The grains maintain the original ellipsoidal shape and have a similar average aspect ratio of 1.2 as the untreated film shown in Figs. 1a and 1b.

Further annealing of the Pd thin film to 32 h gives the microstructure shown in Figs. 4c and 4d. The surface of the film is rougher (Fig. 4c) due to the increased number of protuberances. As the density of the protuberances increases, their average size increases to ~110 nm while the shape becomes less globular and more irregular. Figure 4d shows the necking between the Pd grains, indicating that the agglomerated grains forming the hillocks are starting to sinter. The grain structures on the flat film surface are also partially sintered making it difficult to estimate the average grain size of the film.

The microstructure of the film after 60 h of annealing in He is shown in Figs. 4e and 4f. The large-scale (2000 nm) image of the

FIG. 4. Large and small scale STM images of the film structure: (a, b) after 6 h, (c, d) 32 h, and (e, f) 60 h of He treatment at 523 K.

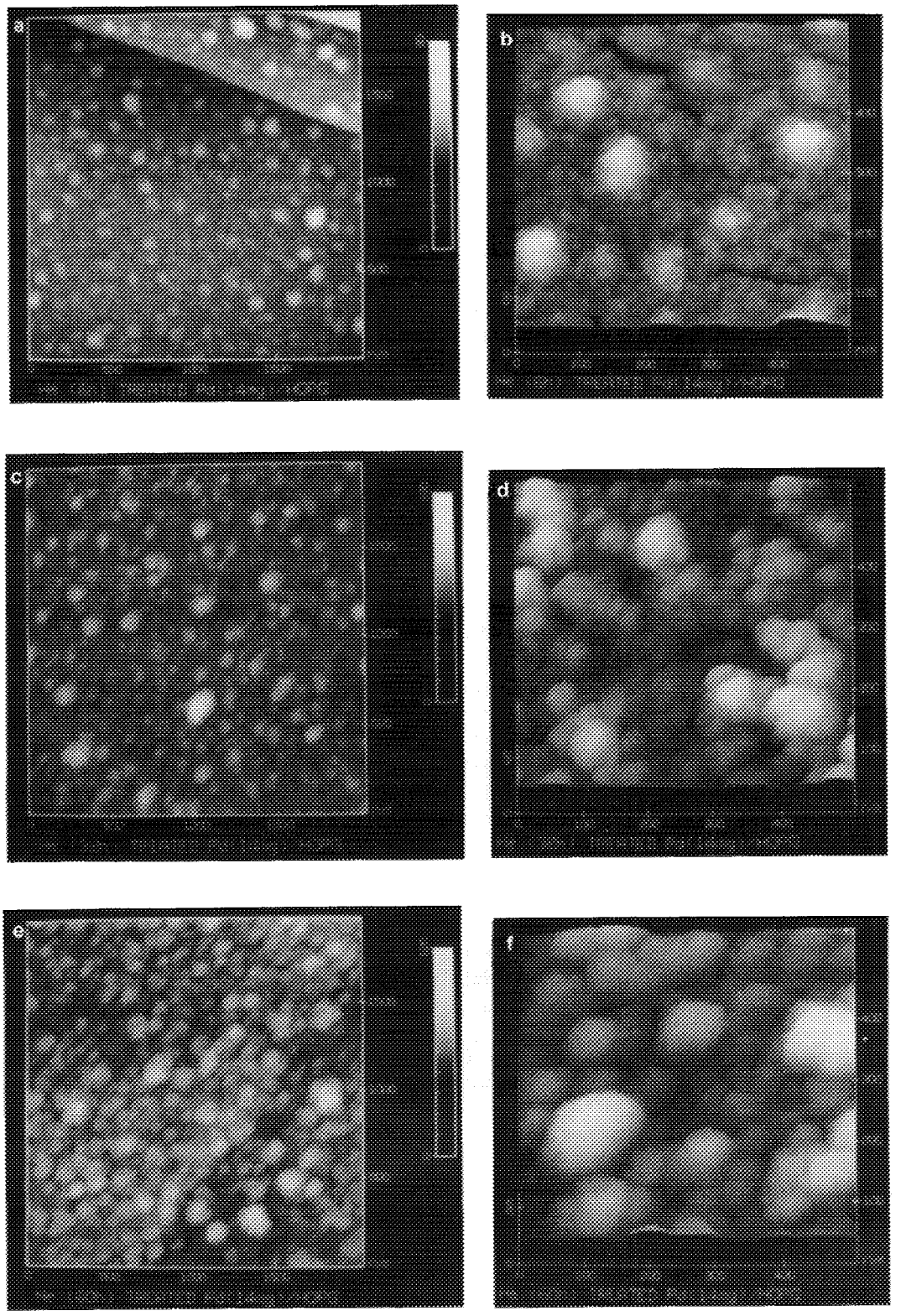
a
b
c
d
e
f

film (Fig. 4e) shows that the film is made up of large sintered grains; ~60% of the particles have a size of 80 × 50 nm (aspect ratio of 1.6) and ~40% are 110 × 95 nm (aspect ratio of 1.2), giving an average size of 92 × 68 nm and an average aspect ratio of 1.4. Figure 4f shows that the large Pd particles sit on top of the relatively flat mosaic floor of Pd grains forming the film surface. These two different surface features indicate that these particles have been formed by the sintering of the agglomerated grains in the "hillocks" observed in Fig. 4b, while the mosaic floor is formed from the flat regions of the film. The other common structure observed in this film is formed by the end to end sintering of the Pd grains forming elongated structures with an average size of 162 × 76 nm and an average aspect ratio of ~2.2.

III. Effect of C_4 Hydrocarbons on the Film Microstructure

The effect of the C_4 hydrocarbons on the film microstructures was also studied. The three hydrocarbons used in this study were *n*-butane, 1-butene, and 1,3-butadiene. Only low concentrations of the hydrocarbons were used to minimize the amount of carbon deposited on the catalyst's surface. The partial pressure of the hydrocarbons under a reactor pressure of 1 atm was maintained at 4 Torr with nitrogen as the diluent gas. The Pd film catalyst was exposed to the hydrocarbons at the preselected temperatures of 348 K for 90 min and subsequently to 473 K for another 90 min, and the resulting film microstructures were analyzed with the STM.

n-Butane. The original grain structure of the deposited Pd thin film (Figs. 1a and 1b) evolved into the structures shown in Figs. 5a and 5b after exposure to 4 Torr of *n*-butane/nitrogen mixture at 348 K for 90 min. Figure 5a shows that the film is made up of oblong Pd grains with an aspect ratio of 2. A smaller scale image (Fig. 5b) shows that the original ellipsoidal grains found on the freshly deposited films had sintered end to end forming the oblong grains. Some of the grains in the Fig. 5b have a "dumbell-like" shape, showing two partially sintered, ellipsoidal grains connected by a neck of material where they touched. Most of the changes observed are limited to the grain structure, with the large-scale film microstructure remaining relatively unchanged, and similar to that of the starting film.

Subsequent exposure of the film to the hydrocarbon at 473 K for another 90 min gives the microstructures shown in Figs. 5c and 5d which display both the structure of the film surface and along its thickness. Figure 5c shows that although the average grain size (17 nm) is close to that of the fresh film, the grains are peculiarly arranged in an end-to-end fashion forming long well defined structures that gives the surface a stringy appearance. The structure of the grain along the thickness of the film (Fig. 5d) shows that as the surface structure becomes more organized, the layers of grains across the film thickness have also sintered to form columnar grain structures.

1-Butene. Exposure of the freshly deposited film to 4 Torr of 1-butene/nitrogen mixture at 348 K for 90 min resulted in minimal changes in the film microstructure with similar, close-packed grain structures as observed in the starting film (Figs. 1a and 1b). Further exposure of the film to the 1-butene hydrocarbon at a higher temperature of 473 K for another 90 min gives the microstructures shown in Fig. 6. The formation of peculiar "Y-shaped" structures on the film surface is shown in Fig. 6a. This image also shows that the surface is covered by a layer of surface deposits. At a higher magnification (Fig. 6b), the "Y-shaped" structures are surrounded by amorphous deposits. These are similar to that of deposited carbons found in previous research.

1,3-Butadiene. The film structure after exposure of the deposited film to 4 Torr of 1,3-butadiene/nitrogen mixture at 348 K for 90 min shows no changes in the film structure, and reexposing the film to the 1,3-butadiene at a higher temperature of 473 K for another

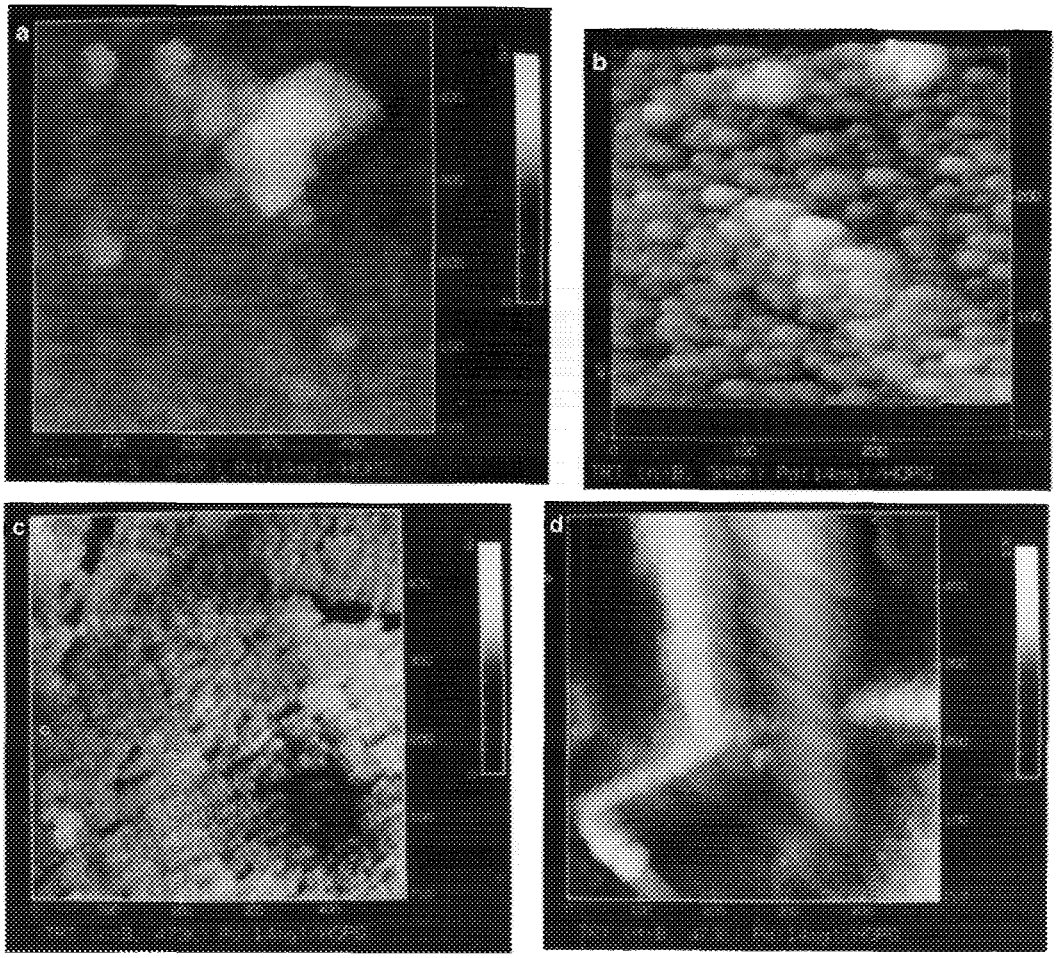

FIG. 5. STM images of the film structure after exposure to *n*-butane/nitrogen mixture at (a, b) 348 K and (c, d) 473 K.

90 min does not have any significant effect, either. Both films are structurally similar to that of the original film (Figs. 1a and 1b) with a measured grain size of 18 nm, which is, within experimental error, the same as that of the original grain size.

IV. Effect of Surface Reaction on the Film Microstructure

The Pd thin film catalyst was also exposed to the reactive mixture of hydrogen and C_4 hydrocarbons to study the effect of the surface reaction on the film microstructure. The partial pressures of the reactant mixture were fixed at 4 Torr of hydrocarbon to 500 Torr of hydrogen and the balance was made up of nitrogen (256 Torr) to give an overall flowrate of 110 ml/min and a H_2/HC ratio of 125. Ranked in the order of increasing reactivity toward hydrogenation, the three hydrocarbons used were *n*-butane, 1-butene and 1,3-butadiene. The evolving film microstructure during the reaction was also studied with respect to the reaction temperature. The Pd film catalyst was allowed to react at each of the preselected temperatures (348, 423, and 473 K) for 90 min and the resulting film structures were analyzed with the STM.

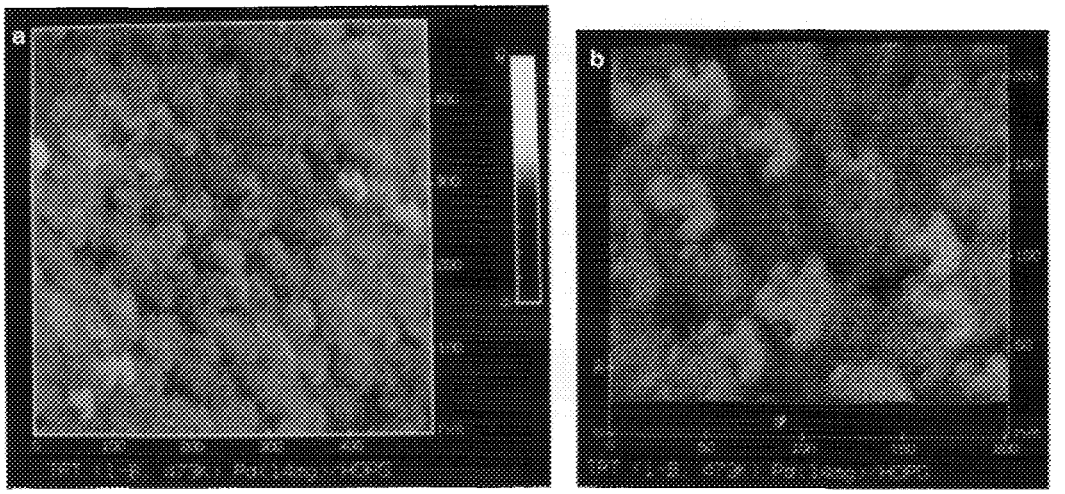

FIG. 6. (a, b) Medium and small scale STM images of the film structure after exposure to 1-butene/nitrogen mixture at 473 K.

The maximum reaction temperature used in the study was fixed at 473 K to prevent excessive carbon formation on the catalyst surface.

n-Butane. A fresh Pd film was exposed to a mixture of *n*-butane and hydrogen gases at a temperature of 348 K for 90 min and the resulting film structure is shown in Figs. 7a and 7b. Both the size and geometry of the Pd grains were modified during the exposure to the gas mixture (Fig. 7a). The initial ellipsoidal grains are transformed into a rectangular shape with an accompanying increase in the average grain size from 15 to 49 × 39.6 nm. The surface of the film is relatively flat and is formed by a mosaic of well ordered rectangular grains. The surface of the rectangular grains (Fig. 7b) is covered by a layer of amorphous deposits, presumably some type of carbons formed by the excessive dehydrogenation of the *n*-butane over the Pd surface.

After the STM analysis, the Pd film was reexposed to the hydrocarbon mixture at a higher temperature of 423 K for another 90 min. The structure of the film had undergone a large change in both the grain and film structure. The rectangular grains had disappeared and were replaced by oblong grains with an average size of 46 nm, with the actual grain size ranging between 20 to 60 nm. The film exhibits nanometer roughness due to the broad size distribution of the grains and the extensive sintering of the grain structure, as shown in Fig. 7c. The film surface appears to be covered by a layer of deposits similar to that observed on the surface of the rectangular grain (Fig. 7b). Figure 7d shows that the surface of the oblong grains is covered by a layer of amorphous deposits that appears as noise in the STM images. After the analysis, the same STM tip was used to image the surface of a fresh Pd film and the grain surface of the film does not have the noise observed in Fig. 7d. In addition, the tip is able to resolve the atomic structure of the underlaying graphite through a crack in the film showing that the noise is due to the surface deposits formed during the film treatment rather than a tip effect. Images of the film after exposure to higher temperature of 473 K show a featureless surface with significant background noise. To eliminate possibility of a faulty tip, a new tip was used to image the sample and similar results were obtained. This is presumably caused by a thick layer of surface deposits formed during the reaction

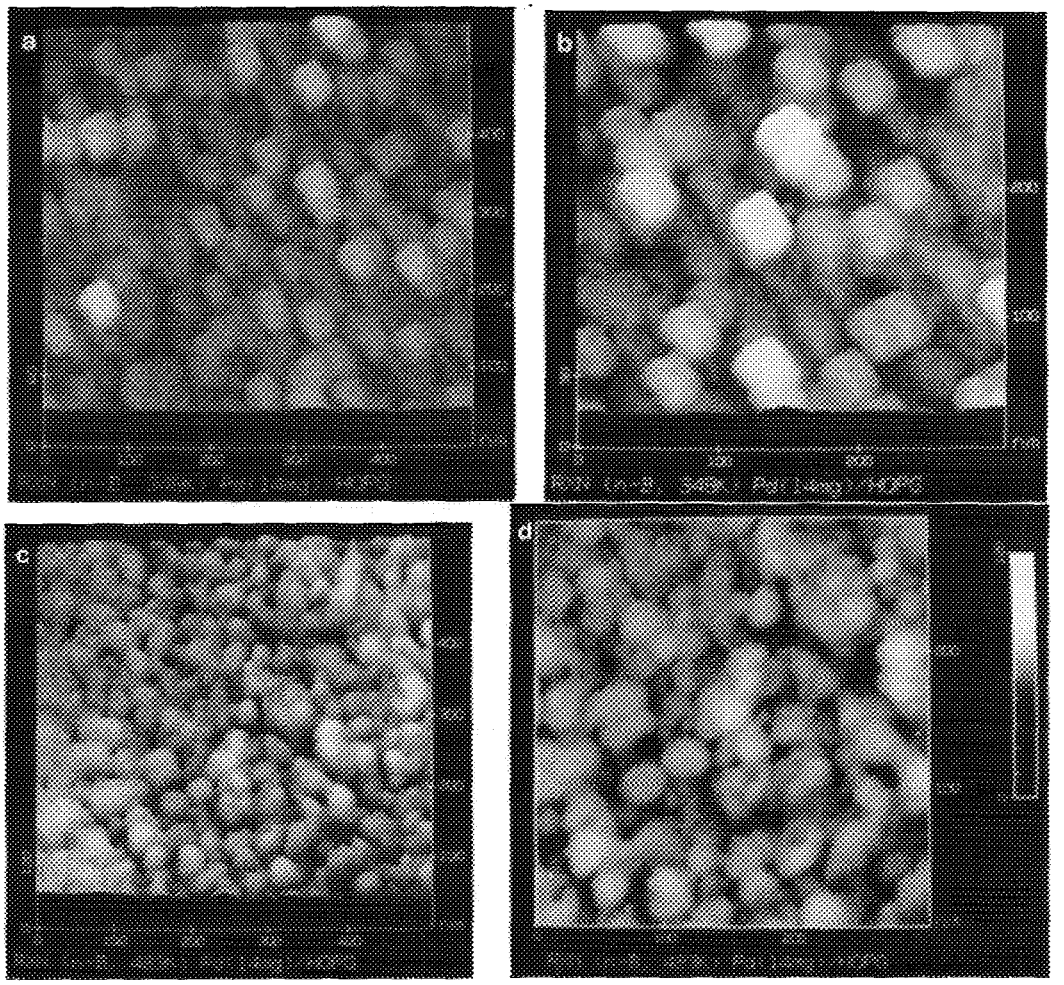

FIG. 7. STM images of the film structure after exposure to the reactant mixture of *n*-butane/hydrogen at (a, b) 348 K and (c, d) 423 K.

which interferes with the STM signal resulting in image deterioration.

1-Butene. Exposure of the freshly deposited Pd film to the reactant mixture of 1-butene and hydrogen at a reaction temperature of 348 K for 90 min has no significant effect on the film structure. The film remains identical to the starting film (Figs. 8a and 8b) with a similar dense surface structure of randomly packed Pd grains. The measured average grain size is 17 nm with an aspect ratio of 1.2. There is no observable 1-butene reaction at this low reaction temperature.

Subsequent reaction of the film at 423 K for another 90 min yielded the film structures shown in the Figs 8c and 8d. Figure 8c shows that the Pd grains become larger and more rounder in shape. The average size of the grains measured from the STM images is 31 nm and the average aspect ratio is 1.1. Through a groove on the surface of the film (Fig. 8d), three layers of grain structures can be observed. The first two layers are relatively flat and are made up of the round grains mentioned above, however, the bottom layer appears to have the same structure as that of Figs. 1a and 1b with a measured grain size of 16 nm.

Further treatment of the film at a higher temperature of 473 K for another 90 min resulted in an increase in the surface roughness of the film. The surface roughness (Fig. 8e) is caused primarily by the broadening of the size distribution of the Pd grains as they began to grow and sinter, however the random packing of the grains also contributes to the overall surface roughness. Figure 8f shows a high magnification image of the film's surface showing the inherent roughness in the surface structure of the Pd grains. A small but significant amount of *n*-butane is formed at temperatures above 398 K; even at 473 K, the amount of 1-butene conversion is only ~7%, attesting to the low reactivity of the 1-butene toward hydrogenation.

1,3-Butadiene. The Pd film sample used for the reaction had the same initial microstructure as that shown in Figs. 1a and 1b. Exposure of the film to the reactant mixture of 1,3-butadiene and hydrogen at a reaction temperature of 348 K for 90 min yielded hydrogenated products (1-butene, *cis*- and *trans*-2-butenes) and results in the formation of facet-like structures in a large area of the Pd film as observed in Figs. 9a and 9b. These structures are rectangular in shape with rounded ends and a measured size of 350 × 200 nm. They are made up of sintered grains, the structures of which can be clearly seen from the STM images. In addition, surface decorations by small, round particles were also observed. In the other regions of the film, the film structure is similar to that of the original film shown in Figs. 1a and 1b, except that the average grain size is 110 instead of 15 nm.

Further reaction of the film at 423 K results in the disappearance of the facet-like structures and the formation of a porous film (Figs. 9c and 9d). Figure 9c shows that the porosity of the film is primarily due the openings in the film structure, and the formation of particles on the film surface. The smaller size of the particles and the grains (~175 nm) suggests that the film had ruptured and redispersed. Although the increased film porosity due to the tears and holes opens up the film microstructure, there is only a limited degree of film fragmentation and the reacted film remains largely continuous with an essentially compact structure.

Sintering of the film was observed after the hydrogenation reaction at 473 K leading to the extensive formation of clusters as shown in Figs. 9e and 9f. Figure 9e shows that the oblong clusters have a relatively large size of 250 nm and an aspect ratio of 1.4. The film is fragmented in several places and it is no longer continuous, thus exposing the underlaying graphite substrate. The measured film thickness is ~50 nm, which is twice as thick as the starting film indicating a probable coalescence of the film. Figure 9f shows that each of the oblong clusters are made up of sintered Pd grains which give it a cauliflower-like surface structure.

The hydrogenation of 1,3-butadiene is very reactive on the Pd film catalyst and even at room temperature, there is a significant butadiene conversion. Measuring the catalyst's reactivity at 323 K before and after the exposure of the film to the reactant mixture permits one to trace the history of catalyst activity as the film microstructure evolves. The butadiene conversion at 323 K for $H_2/HC = 125$ is plotted against the treatment temperature of the film as shown in Fig. 10. The plot shows that the initial film structure has a low reactivity toward 1,3-butadiene and the formation of facet structures coincides with the decline in the reactivity. A large increase in the reactivity accompanies the rupturing of the film and formation of the cauliflower-like clusters.

FIG. 8. STM images of the film structure after exposure to the reactant mixture of 1-butene/hydrogen at (a, b) 348 K, (c, d) 423 K, and (e, f) 473 K.

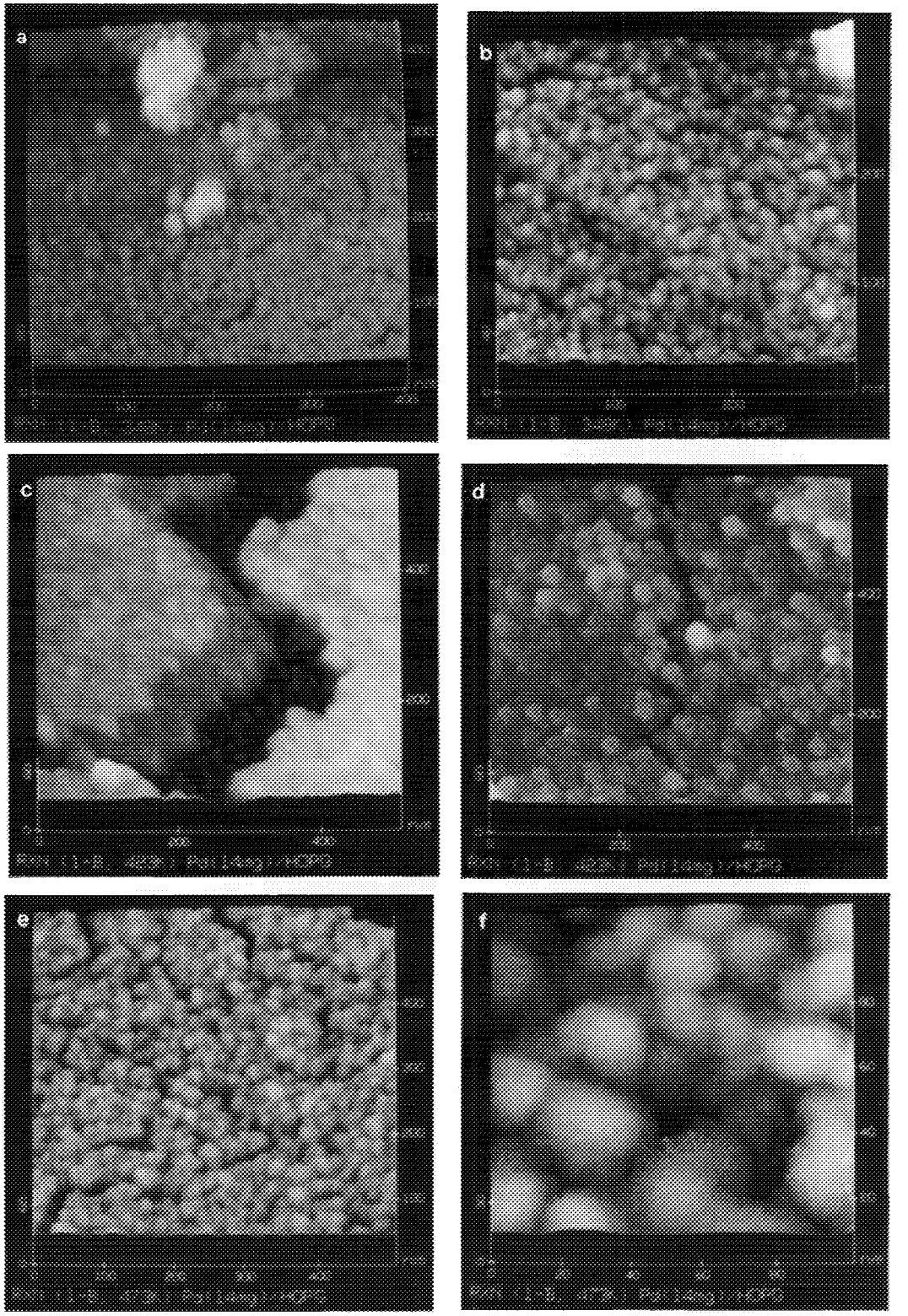
a
b
c
d
e
f

This period of rapid evolution of film microstructure from that of the fresh film to the formation of the clusters coincides with a two- to threefold increase in reactivity and is termed the activation period of the film catalyst. The behavior of the activity plot in Fig. 10 shows that the activation and deactivation processes on the film catalyst accompanies the transformation of the film microstructure during the hydrogenation reaction.

DISCUSSION

I. Evolution of Film Microstructure during H_2 Treatment

The fresh catalyst, although prepared by a standard evaporation technique, was not annealed prior to the treatment studies. Furthermore, the substrates were not heated during the deposition which resulted in the rapid condensation of Pd aggregates formed during the evaporation, thus giving the film a grainy structure. Such structures are likely to be less stable than if annealed and rather susceptible to the transformations described in the results section. Like all surfaces, the thin film catalyst tries to achieve an equilibrium microstructure that minimizes the total surface free energy of the system which is only limited by the kinetics of the surface processes involved. To reach an equilibrium microstructure, the surface has to evolve through a series of increasingly stable microstructures (*14*). At sufficiently low temperatures, the structural transformation is slow, and these quasi-stable microstructures can be analyzed as in the hydrogen treatment study. This allows one to obtain snapshots of the surface transformation as it evolves. This is important in elucidating the details of the dynamic processes taking place.

During the early stages of H_2 treatment (up to 6 h), the continuous growth in the grain size is similar to the normal grain growth (*15*) described in the previous annealing study by Chopra and Bobb (*16*) and Vook and Witt (*17*). The flux of materials from one region of the surface to another can be due to the difference in the size of the neighboring grains (*18*) or due the curvature of the surface (*14*, *19*). Mullins (*14*) has shown that the chemical potential of surface atoms is dependent on the surface curvatures, and is responsible for a number of capillarity effects in morphological changes (*20*, *21*). Growth stagnation also referred to as specimen thickness effect had been reported by Sperry and co-workers (*22*) for the Al–Mn thin film alloys and by Smith and co-workers (*23*) for a germanium thin film. Growth stagnation occurred when the average grain size was about two to three times the thickness of the film as it was in this study. Grain growth was not limited to two-dimensions and also occurred along the film thickness (*24*). At the stagnation point, the boundaries of the grain had completely traversed the thickness of the film, giving the grain a columnar structure which was also observed in this study (Fig. 1f). This and the agglomeration of the grain (Fig. 1e) can cause stresses along the film–substrate interface resulting in film deformation and buckling giving rise to the chain-like structures observed in Figs. 1e and 1f.

Thompson and collaborators (*25*) have shown that growth beyond the stagnation point is achieved by abnormal grain growth with rapid outward migration of the grain boundaries. The grain size distribution passes through a bimodal phase, then back to a monomodal distribution as the normal grains are consumed by the abnormal grains (*15*). In this study, after 32 h of treatment, grain sintering results in structural changes

FIG. 9. Large and medium scale STM image of the film structure after exposure to the reactant mixture of 1,3-butane/hydrogen at (a, b) 348 K, (c, d) 423 K, and (e, f) 473 K.

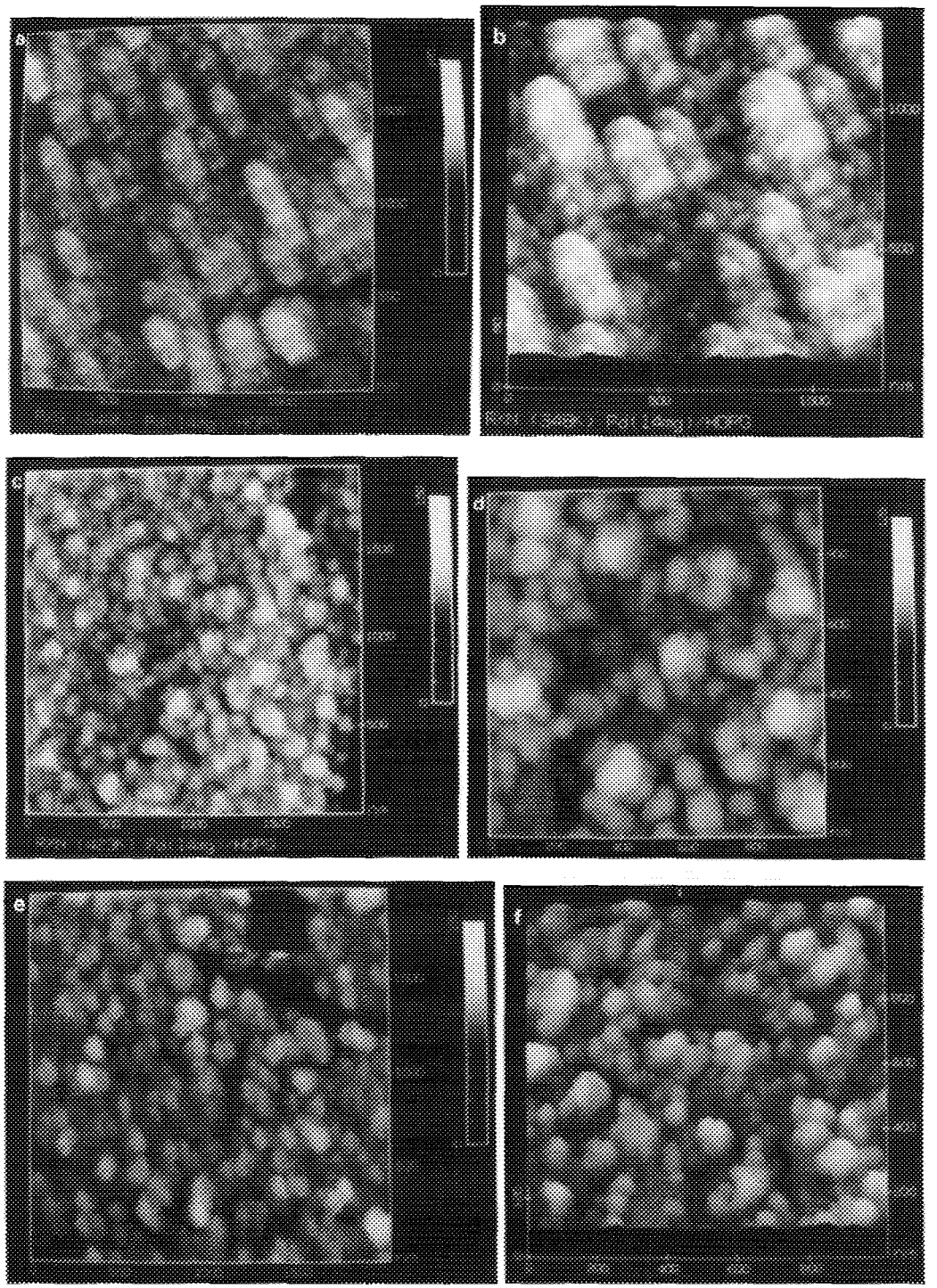
a
b
c
d
e
f

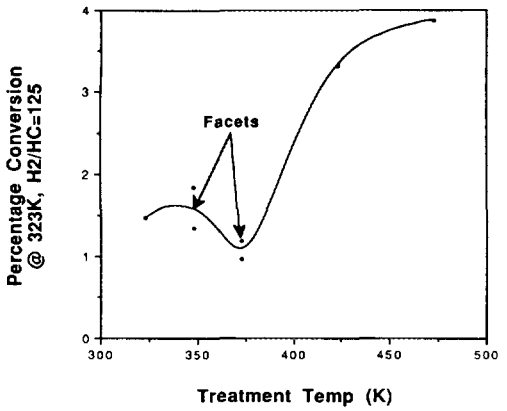

FIG. 10. The 1,3-butadiene conversion measured at 323 K for the different film structure obtained at different treatment temperatures.

and in a sudden increase in the grain size. Along with sintering, facet-like structures were also formed giving the film a bimodal structure. Large, elongated facets (Figs. 3a and 3b) cover most of the film surface after 48 h of treatment in hydrogen.

Up to this point, the growth in the grain size and formation of facet structures are in agreement with both experimental (*26*) and modeling results (*27*, *28*) for various thin film systems. However, as the facet grows by sintering, the strains accumulated due to the mismatches in the grain lattices are relieved through film rupture. Film rupture can also be the result of thermal stress caused by temperature cycling (heating and cooling), however, a study of a film treated uninterruptedly for 60 h shows an identical microstructure as that of Figs. 3c and 3d. In addition, the treatment temperature was relatively low at 523 K (250°C). It is important to note that prior to rupture, the film structure is constrained mainly to two dimensions. Film rupture does not only relieve the film stress but also allows the film greater degree of freedom. Further H_2 treatment only resulted in the resintering of the film with subsequent formation of large, 3-D particles among the fragmented films. Rupture and redispersion of metal particles was observed by Ruckenstein and collaborators for Pt/alumina (*29*) and in the previous study by the authors on supported Pt particles (*30*).

II. Gas-Induced Structural Transformations

Hydrogen and helium gases. The results of the hydrogen, helium, and C_4 hydrocarbon treatment studies show that the different gases have different effect on the surface morphology of the Pd/HOPG thin film. Shi and Masel (*31*) had shown that the surface orientations with the strongest interaction with the adsorbate will preferentially grow and form facets. Likewise, the adsorbate gas with the strongest interaction with the surface will cause the greatest changes in the surface structure as observed in the study. Helium is an inert gas and can only physisorb on the palladium surface, whereas at the temperature used, hydrogen molecules chemisorb and dissociate on the surface of palladium forming adsorbed hydrogen atoms. Palladium can also absorb hydrogen to form palladium hydride (*27*). This explains why the Pd film exhibits greater structural change during the hydrogen treatment than in a similar helium treatment. The absorbed hydrogen undoubtedly plays a role in the observed changes in the microstructure, although they cannot be isolated from those induced by the chemisorbed hydrogen.

C_4 hydrocarbons. The effect of the C_4 hydrocarbons (*n*-butane, 1-butene, and 1,3-butadiene) on the film structure at two different temperatures shows that at low temperatures, the film exposed to *n*-butane exhibited some sintering in the grain structure, however, the films exposed to the 1-butene and 1,3-butadiene did not exhibit any significant change in film structure. At higher temperatures, the film exposed to *n*-butane showed extensive grain sintering. Excessive carbon deposition and formation of peculiar Y-shaped structures were observed in the film exposed to 1-butene, while the film exposed to 1,3-butadiene remained the same.

For the C_4 hydrocarbons, the structural changes in the Pd thin film coincides with

the appearance of products at elevated temperature: 1-butene for *n*-butane and carbon for 1-butene. Sequential dehydrogenation of 1-butene can occur on Pt and Pd, and it may explain the increase in the amount of carbon deposits with increasing treatment temperature (*32*, *33*). Conjugated dienes such as 1,3-butadiene are more stable than the alkenes (*34*), and no reaction products or carbon deposit were observed at either high or low temperature. The structural changes from the original film increase with the severity in the observed *n*-butane and 1-butene dehydrogenation. On the other hand, the 1,3-butadiene does not exhibit any reaction and the starting film structure was preserved. Therefore, the presence of surface reaction has a greater effect on the surface structure of the Pd film than in the presence of the adsorbate alone.

C_4 hydrocarbons and hydrogen gas mixture. Olefin products in the form of 1-butene and 2-butenes were obtained during the exposure of the film catalyst to *n*-butane/hydrogen mixture, indicating butane dehydrogenation. The observed surface structural changes coincided with the appearance of reaction products. In addition, the STM images also show an increasing carbon deposition on the film surface, such that at 473 K most of the film is covered with carbon, hiding most of the surface features. The well ordered, rectangular grains observed during the film's exposure to *n*-butane/hydrogen mixture at 348 K were not observed in either hydrogen treatment or during exposure to *n*-butane. This is due to the fact that during exposure to butane/H_2 the reaction environment is different from that of hydrogen or *n*-butane.

The conversion is low during the 1-butene hydrogenation over the Pd thin film. Most of the structural changes observed by STM are small and confined to the grain structure of the film which grows continuously from 17, to 31, to 35 nm with increasing temperature. Among the three C_4/H_2 feeds studied, the 1,3-butadiene has the highest activity toward hydrogenation and exhibits the greatest structural change.

The reaction results show that the presence of a surface reaction, either hydrogenation or dehydrogenation, has a greater effect on the film microstructure than in the absence of reaction. In all three cases, the surface morphology obtained in the presence of a hydrocarbon/hydrogen mixture is different from that of hydrogen treatment or exposure to the hydrocarbon alone. The structural changes during reaction are likely to be due to the combined effects of the two adsorbed reactants, hydrogen and hydrocarbon. Furthermore during the reaction, reaction intermediates, hydrocarbon fragments, and carbon deposits are also formed on the catalyst surface and it is very likely that they contribute to the structural changes.

Structural transformations occur at a faster rate in the presence of 1,3-butadiene hydrogenation than in hydrogen. To obtain a similar film structure as that in Figs. 9e and 9f requires exposure of the film for 7.5 h in C_4H_6/H_2 gas mixture at an average temperature of 373 K compared to 60 h in H_2 at 523 K. Local heating generated by the heat of reaction can also increase the rate of structural transformation. The butadiene hydrogenation reaction is exothermic with ΔH_r ranging between 22.52 to 50.29 kcal/gmol depending on the extent of hydrogenation, i.e., butenes or *n*-butane, respectively.

In this study, the repeated exposure of the thin film to air during the STM analysis is of major concern. Oxygen and water present in the air can have a major effect on the film microstructure. Precautions were taken to flush the catalyst with Ar or N_2 (~30 min) prior to heating to remove oxygen and water from the film, however, this does not entirely preclude the presence of submonolayer oxygen and water adsorbates on the surface. Additional experiments were also done in which the structure of the uninterrupted H_2 treated film (48 h) without O_2 exposure was found to be similar to that shown in Figs. 3a and 3b.

In the presence of the hydrocarbons, carbon contaminants from the reaction byprod-

uct can not be avoided and their presence on the film can have a direct effect on the surface morphology of the Pd film. However, if all the structural changes in the film are due primarily to the carbon deposits, then the underlaying film structures for all three hydrocarbons will be similar, which is not the case, since exposure to each of the C_4 hydrocarbons results in different structural changes. No carbide or graphite formations is expected due to the low temperatures used in the study. The conditions during the H_2 treatment and hydrogenation reaction do not exclude probable hydride formation due to large excess of hydrogen partial pressure, and may be responsible for some of observed structural transformations.

CONCLUSIONS

The effect of the hydrogen and helium treatment on the structural transformation of the Pd thin film catalyst supported on the HOPG has been investigated with STM. The evolving film microstructures during H_2 treatment shows the dynamic nature of the thin film catalyst, from the initial growth of the grain size, followed by sintering and facet formation, then by facet growth, and its eventual disappearance through rupturing. The study also shows that the strong interaction between the Pd surface and the hydrogen resulted in a greater structural changes than in helium indicating that the hydrogen has a stronger effect on the film structure than the relatively inert helium.

The effect of the C_4 hydrocarbons (*n*-butane, 1-butene, and 1,3-butadiene) and treatment temperature on the thin film microstructure was also examined. Similarly, the presence of a surface reaction due to the catalytic action of the Pd surface has a greater effect on the film structure than the adsorbates alone. To further clarify the effect of the reaction on the film microstructure, a mixture of dilute C_4 hydrocarbons in excess hydrogen (diluent = nitrogen) was reacted over the thin film catalyst at various temperatures for 90 min. The presence of surface reaction, either hydrogenation (1-butene and 1,3-butadiene) or dehydrogenation (*n*-butane) resulted in a significant modification of the film structure at both large and small scales. The more reactive hydrocarbons, 1,3-butadiene and *n*-butane affect a greater structural change than the less reactive hydrocarbon, 1-butene. Comparison of the results from the H_2 treatment and 1,3-butadiene hydrogenation shows that the presence of reaction has a greater effect on the structure than the hydrogen alone. Therefore, the presence of a surface reaction, either the dissociation of hydrogen or hydrogenation and dehydrogenation of C_4 hydrocarbons, have a greater influence on the film structure than the adsorbate-surface interaction. The results also show that the change in the structure during the 1,3-butadiene hydrogenation is accompanied by a change in the intrinsic activity of the thin film catalyst, indicating a strong dependence of the catalytic activity and selectivity on the microstructure, which shall be the major topic of a second paper.

ACKNOWLEDGMENTS

Funds to purchase the equipments were provided by NSF CBT 88-06640 and the research was funded by NSF CTS 90-01586.

REFERENCES

1. Baratoff, A., Binnig, G., Fuchs, H., Salvan, F., and Stoll, E., *Surf. Sci.* **168,** 734 (1986).
2. Wintterlin, J., Wiecher, J., Brune, H., Gritsch, T., Hofer, H., and Behm, R. J., *Phys. Rev. Lett.* **62,** 59 (1989).
3. Kuk, Y., and Silverman, P. J., *J. Vac. Sci. Technol. A* **8,** 289 (1991).
4. Ogletree, D. F., Hwang, R. Q., Zeglinski, D. M., Lopez Vazquez de-Parga, A., Somorjai, G. A., and Salmeron, M., *J. Vac. Sci. Technol. B* **9,** 886 (1991).
5. Denley, D. R., *J. Vac. Sci. Technol. A* **8,** 603 (1990).
6. Erlandsson, R., Eriksson, M., Olsson, L., Helmersson, U., and Lunstrom, I., *J. Vac. Sci. Technol. B* **9,** 825 (1991).
7. Buchholz, S., Fuchs, H., and Rabe, J. P., *J. Vac. Sci. Technol. B* **9,** 857 (1991).
8. Ganz, E., Sattler, K., and Clarke, J., *Phys. Rev. Lett.* **60,** 1856 (1988).
9. Humbert, A., Dayez, M., Granjeaud, S., Ricci,

P., Chapon, C., and Henry, C. R., *J. Vac. Sci. Technol. B* **9,** 804 (1991).
10. Yeung, K. L., and Wolf, E. E., *J. Catal.* **135,** 13 (1992).
11. Yeung, K. L., and Wolf, E. E., *Catal. Lett.* **12,** 213 (1992).
12. Yeung, K. L., and Wolf, E. E., *J. Vac. Sci. Technol. B* **9,** 798 (1991).
13. Yeung, K. L., and Wolf, E. E., *Appl. Catal.*, in press.
14. Mullins, W. W., *in* "Metal Surfaces: Structure, Energetics and Kinetics" (W. D. Robertson and N. A. Gjostein, Eds.), pp. 17–66. ASM, Metal Park, OH, 1962.
15. Frost, H. J., *in* "Evolution of Thin-Film and Surface Microstructure" (C. V. Thompson, J. Y. Tsao, and D. J. Srolovitz, Eds.), pp. 115–130. MRS, Pittsburg, PA 1991.
16. Chopra, K. L., and Bobb, L. C., *Acta Metall.* **12,** 807 (1964).
17. Vook, R. W., and Witt, F., *J. Vac. Sci. Technol.* **2,** 243 (1965).
18. Wynblatt, P., and Gjostein, N. A., *Prog. Solid State Chem.* **9,** 21 (1975).
19. C. Herring, *in* "The Physics of Powder Metallurgy" (W. E. Kingston, Ed.). McGraw–Hill, New York, 1951.
20. C. Herring, *in* "Structure and Properties of Solid Surfaces" (R. Gomer and C. S. Smith, Eds.). Univ. of Chicago Press, Chicago, 1952.
21. Kuczynski, G. C., *J. Appl. Phys.* **21,** 632 (1950).
22. Beck, P. A., Holtzworth, M. L., and Sperry, P. R., *Trans. AIME* **180,** 163 (1949).
23. Palmer, J. E., Thompson, C. V., and Smith, H. I., *J. Appl. Phys.* **62,** 2492 (1987).
24. Chopra, K. L., "Thin Film Phenomena." McGraw–Hill, New York, 1969.
25. Wong, C. C., Smith, H. I., and Thompson, C. V., *J. Appl. Phys.* **48,** 335 (1986).
26. Keith, H. D., *Proc. Phys. Soc. London B* **69,** 180 (1956).
27. Palczewska, W., *in* "Hydrogen Effect in Catalysis: Fundamentals and Practical Applications" (Z. Paal and P. G. Menon, Eds.). Dekker, New York, 1988.
28. Soares, A., Ferro, A. C., and Fortes, M. A., *Scr. Metall.* **19,** 1491 (1985).
29. Ruckenstein, E., and Sushumna, I., *in* "Hydrogen Effect in Catalysis: Fundamentals and Practical Applications" (Z. Paal and P. G. Menon, Eds.). Dekker, New York, 1988.
30. Yeung, K. L., and Wolf, E. E., *J. Vac. Sci. Technol. A* **10,** 651 (1992).
31. Shi, A-C., and Masel, R. I., *J. Catal.* **120,** 421 (1989).
32. Paul, J-P., and Sautet, P., *Catal. Lett.* **9,** 245 (1991).
33. Avery, N. R., and Sheppard, N., *Surf. Sci. Lett.* L367 (1986); *Proc. R. Soc. London Ser. A* **405,** 27 (1986).
34. Morrison, R. T., and Boyd, R. N., "Organic Chemistry," 3rd ed. Allyn and Bacon, Boston, 1973.